Science Advances
AAAS

Supplementary Materials for

TENT5 cytoplasmic noncanonical poly(A) polymerases regulate the innate immune response in animals

Vladyslava Liudkovska *et al.*

Corresponding author: Andrzej Dziembowski, adziembowski@iimcb.gov.pl

Sci. Adv. **8**, eadd9468 (2022)
DOI: 10.1126/sciadv.add9468

The PDF file includes:

Other Supplementary Material for this manuscript includes the following:

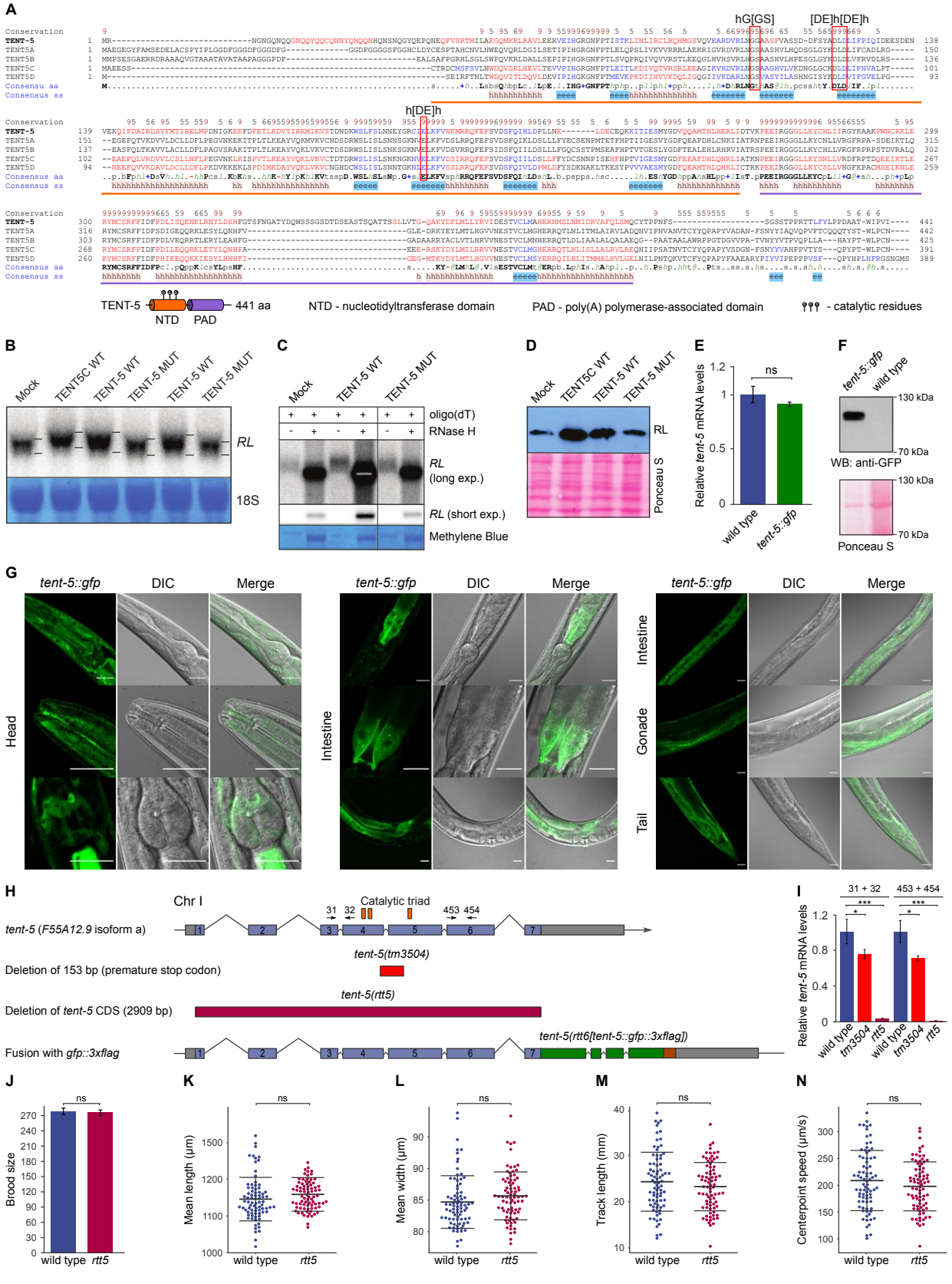
A
hG[GS]
[DE]h[DE]h
h[DE]h
TENT-5
441 aa
NTD
PAD
NTD - nucleotidyltransferase domain
PAD - poly(A) polymerase-associated domain
- catalytic residues
B
Mock
TENT5C WT
TENT-5 WT
TENT-5 MUT
RL
18S
C
oligo(dT)
RNase H
RL (long exp.)
RL (short exp.)
Methylene Blue
D
RL
Ponceau S
E
Relative tent-5 mRNA levels
ns
wild type
tent-5::gfp
F
tent-5::gfp
wild type
130 kDa
70 kDa
WB: anti-GFP
Ponceau S
G
tent-5::gfp
DIC
Merge
Head
Intestine
Gonade
Tail
H
Chr I
Catalytic triad
tent-5 (F55A12.9 isoform a)
Deletion of 153 bp (premature stop codon)
tent-5(tm3504)
Deletion of tent-5 CDS (2909 bp)
tent-5(rtt5)
Fusion with gfp::3xflag
tent-5(rtt6[tent-5::gfp::3xflag])
I
31 + 32
453 + 454
Relative tent-5 mRNA levels
wild type
tm3504
rtt5
J
Brood size
K
Mean length (µm)
L
Mean width (µm)
M
Track length (mm)
N
Centerpoint speed (µm/s)

Fig. S1. TENT-5 is a cytoplasmic ncPAP in worms.

(**A**) upper panel: Multiple sequence alignment of TENT-5 and human TENT5A-D proteins. Residues critical for the TENT5 proteins catalytic activity are marked with red boxes. TENT5 ncPAPs contain NTase domain with catalytic triad ([DE]h[DE]h, h[DE]h) and PAP-associated domain, underlined in orange and violet, respectively, and shown schematically in the lower panel (based on (*25*)). (**B**) Northern blot detection of *RL* reporter mRNA using total RNA from mock-transfected 293T cells or cells transfected with constructs that express NHA-hsTENT5C^{WT} (TENT5C WT, positive control), NHA-TENT-5^{WT} (TENT-5 WT), or NHA-TENT-5^{D151A,D153A} (TENT-5 MUT). Samples from two independent transfections are shown for TENT-5. In the cells transfected with NHA-hsTENT5C^{WT} or NHA-TENT-5^{WT} the *RL* mRNA migrates slowly, indicating its bigger length. Methylene blue staining of 18S rRNA serves as a loading control. (**C**) Northern blot detection of *RL* reporter mRNA using poly(A)+ RNA isolated from 293T cells transfected as in B. Observed differences in *RL* mRNA gel-migration upon tethering of NHA-TENT-5^{WT} resulted from mRNA polyadenylation, as revealed by the fact that *RL* mRNA from mock and NHA-TENT-5^{WT}-transfected cells migrated equivalently following RNA treatment with RNase H in the presence of oligo(dT)$_{25}$. Methylene blue staining serves as a loading control. (**D**) NHA-TENT-5^{WT} tethering increases RL reporter protein levels. Western blot detection of RL from mock-transfected 293 cells or from cells transfected with constructs that express NHA-hsTENT5C^{WT} (TENT5C WT, positive control), NHA-TENT-5^{WT} (TENT-5 WT), or NHA-TENT-5^{D151A,D153A} (TENT-5 MUT). Ponceau S staining serves as a loading control. (**E**) RT-qPCR quantification of *tent-5* mRNA levels in wild-type and *tent-5(rtt6[tent-5::gfp::3xflag] I*) knock-in strain. Data represent mean ± standard deviation (SD) of three biological replicates. ns – not significant (two-tailed t-test). (**F**) Anti-GFP immunoblot blot analysis of total protein lysate prepared from the *tent-5::gfp* worms. Total protein lysate from wild type was used as a negative control. Ponceau S staining of membrane serves as a loading control. (**G**) Representative fluorescence and DIC images of TENT-5-GFP expression. Scale bar is 20 µm. (**H**) Schematic of *tent-5* gene structure and mutant alleles. Exons are depicted as blue (*tent-5*), green (*gfp*), and brown (3x*flag*) boxes, UTRs as grey boxes, introns as lines. The approximate positions of triplets encoding catalytic residues are marked with orange boxes. Arrows correspond to the position of primers used for RT-qPCR. (**I**) RT-qPCR quantification of *tent-5* mRNA levels in L4 wild-type and mutant worms. Data represent mean ± SD of three biological replicates; $*P \leq 0.05$; $**P \leq 0.01$; $***P \leq 0.001$ (two-tailed t-test). (**J**) Total brood size of wild-type and *tent-5*-deficient worms (n=10, average of two independent trials). Data represent mean ± SD; ns – not significant (two-tailed unpaired t-test). Analysis of the worms' body length (**K**) and width (**L**), track length (**M**), and centerpoint speed (**N**) with the WormLab software. 80 young adult worms per strain have been analyzed. Data represent mean ± SD; ns – not significant (two-tailed unpaired t-test with Welch's correction).

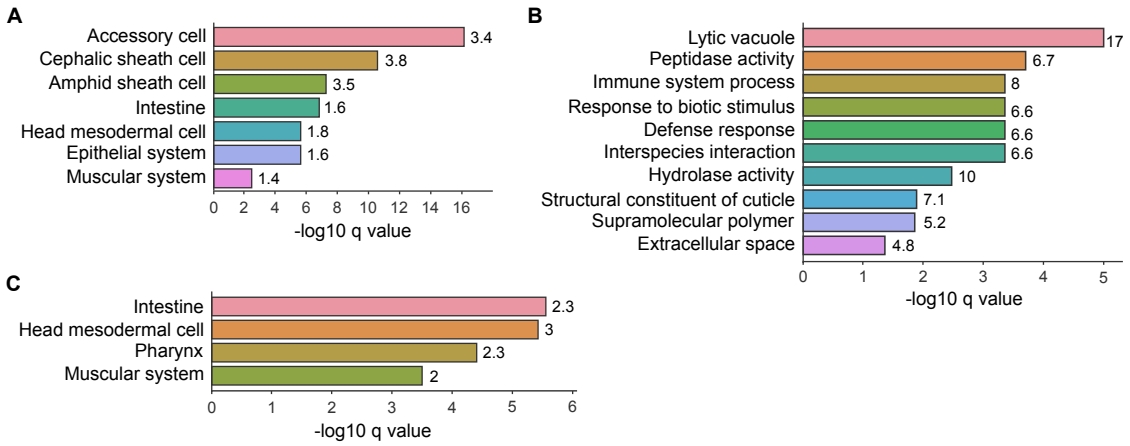

Fig. S2. Loss of *tent-5* leads to the downregulation of genes that encode innate immune effectors. (**A** and **C**) Tissue enrichment analysis of downregulated genes (log2FC < -log2(1.5), RNA-seq) (**A**) and proteins (p value < 0.05, Mass Spectrometry) (**C**) which levels were decreased in *tent-5(tm3504)* mutant compared to the wild-type worms. (**B**) Overrepresented functional GO terms of proteins with decreased abundance in *tent-5*-deficient worms in comparison to the wild type (Mass Spectrometry). Numbers on the right indicate the enrichment fold change for each term (observed/expected genes).

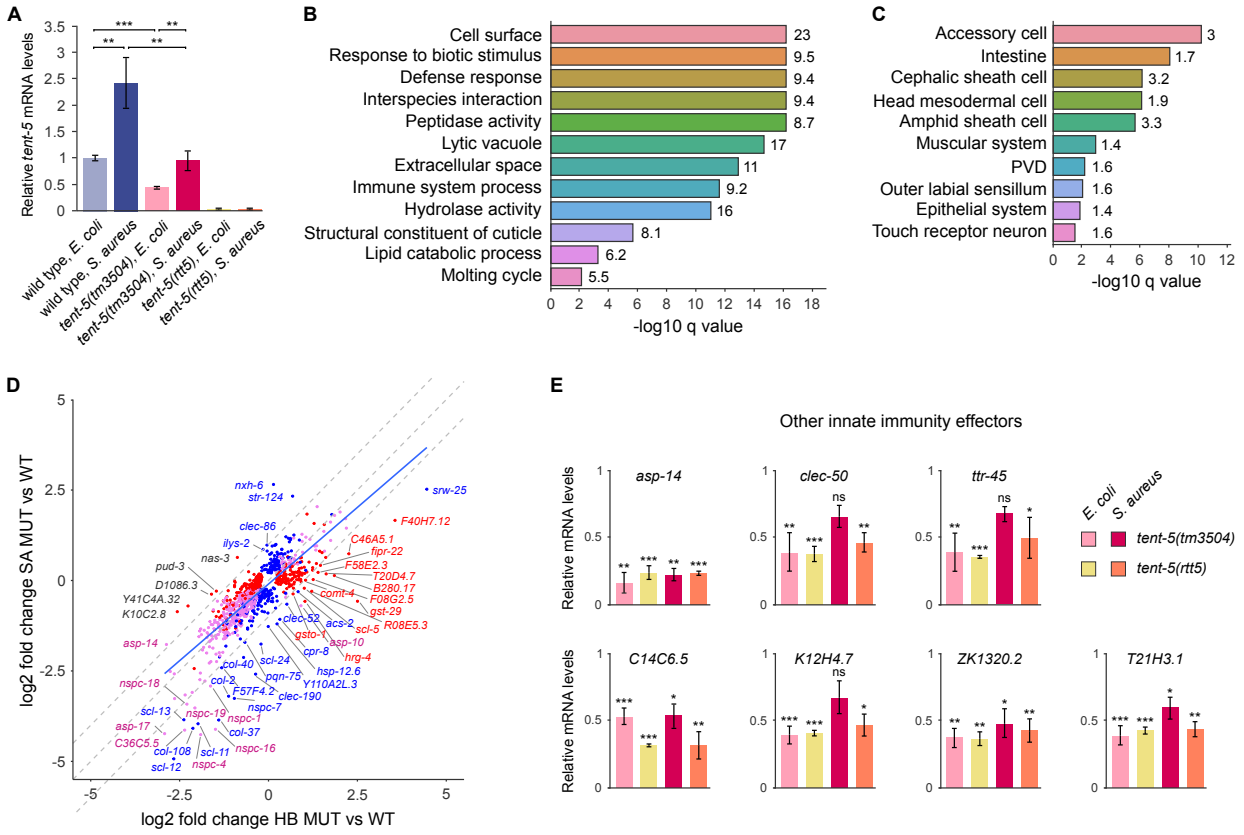

Fig. S3. TENT-5 deficiency leads to the downregulation of genes that encode innate immune effectors. (**A**) RT-qPCR analysis of *tent-5* expression in wild type, *tent-5(tm3504)*, and *tent-5(rtt5)* worms that were exposed to *S. aureus* or control *E. coli* for 8 hours. Relative *tent-5* mRNA level was normalized to *act-1* and wild type. Data represent mean ± SD of three biological replicates; $*P \leq 0.05$; $**P \leq 0.01$; $***P \leq 0.001$ (two-tailed t-test). (**B** and **C**) Overrepresented functional GO and TEA terms of genes downregulated (log2FC < -log2(1.5)) in *tent-5(tm3504)* mutant compared to wild type upon infection of L4 worms with *S. aureus* for 8 hours. Numbers on the right indicate the enrichment fold change for each term. (**D**) Scatter plot illustrates a comparison of the differential expression of genes (|log2FC| > 0, FDR < 0.05) between mutant (MUT) and wild type (WT) in infected (SA) and non-infected (HB) animals. Red and blue dots indicate genes differentially expressed in wild-type and mutant worms, respectively. Dots in magenta indicate the common part. The middle diagonal dashed line shows the equal response of both genotypes, and two additional dashed lines show the borders of the area where the response is +/- 1 log2FC. The solid blue line shows a linear trend created using the linear regression model for all data points. (**E**) RT-qPCR analysis of relative levels of mRNA expression in two *tent-5*-deficient worm strains grown on *E. coli* or exposed to *S. aureus* for 8 hours. Relative abundance of mRNAs was normalized to *act-1* and wild type. Data represent mean ± SD of three biological replicates; ns – not significant; $*P \leq 0.05$; $**P \leq 0.01$; $***P \leq 0.001$ (two-tailed t-test).

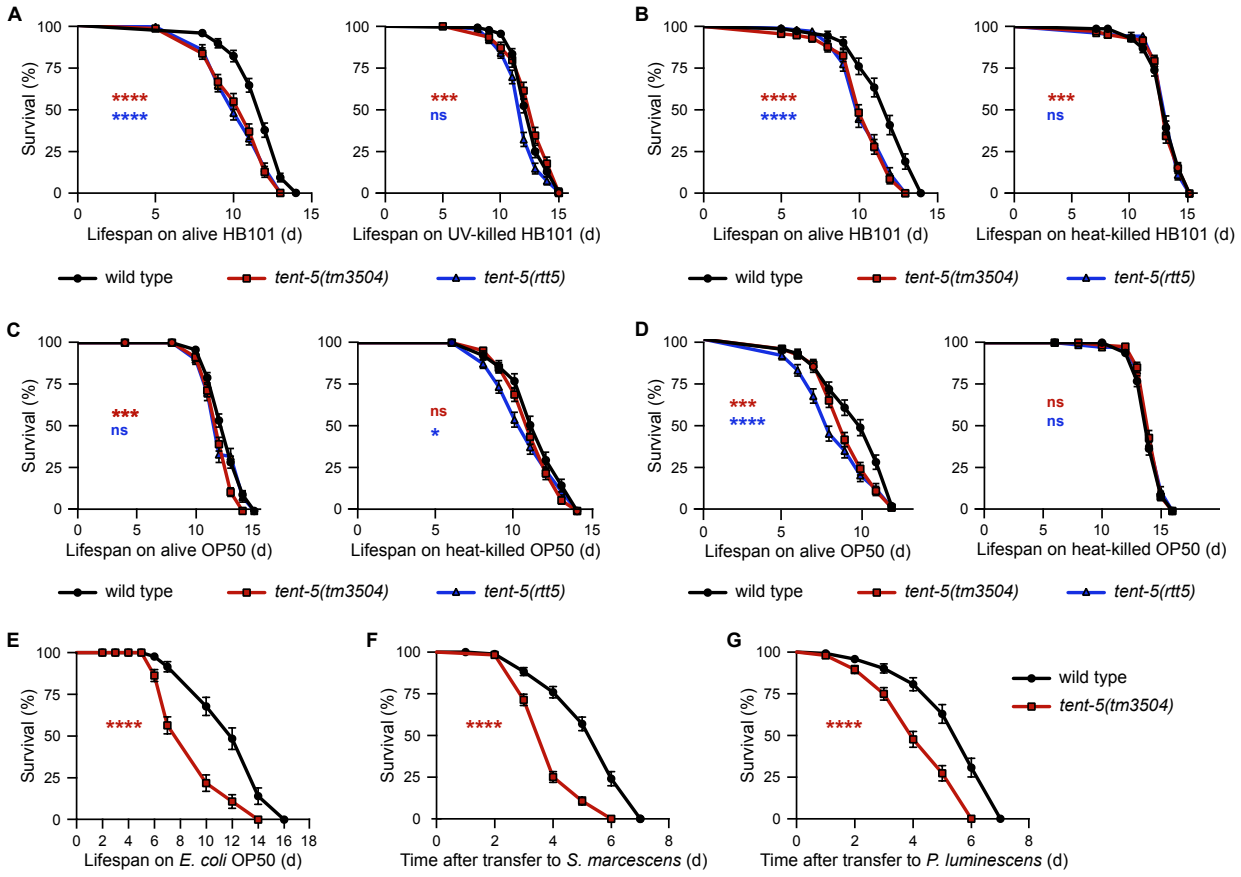

Fig. S4. TENT-5 is required for the host defense against various bacterial strains. (**A-D**) The lifespan of wild type, *tent-5(tm3504),* and *tent-5(rtt5)* worms grown at 25°C on plates seeded with alive or UV-killed *E. coli* HB101 (**A**), alive or heat-killed *E. coli* HB101 (**B**), and alive or heat-killed *E. coli* OP50 (**C** and **D**). For these experiments, NGM plates contained FUdR. **P* < 0.05; ***P* < 0.01; ****P* < 0.001; *****P* < 0.0001; ns – not significant (Log-Rank test). (**E-G**) Survival of wild type and *tent-5(tm3504)* worms grown on *E. coli* OP50 (**E**) or infected with *S. marcescens* (**F**) and *P. luminescens* (**G**). Experiments presented in **E-G** are representative of at least two independent trials; **P* < 0.05; ***P* < 0.01; ****P* < 0.001; *****P* < 0.0001; ns – not significant (Log-Rank test). Survival statistics related to lifespan and survival assays can be found in table S1.

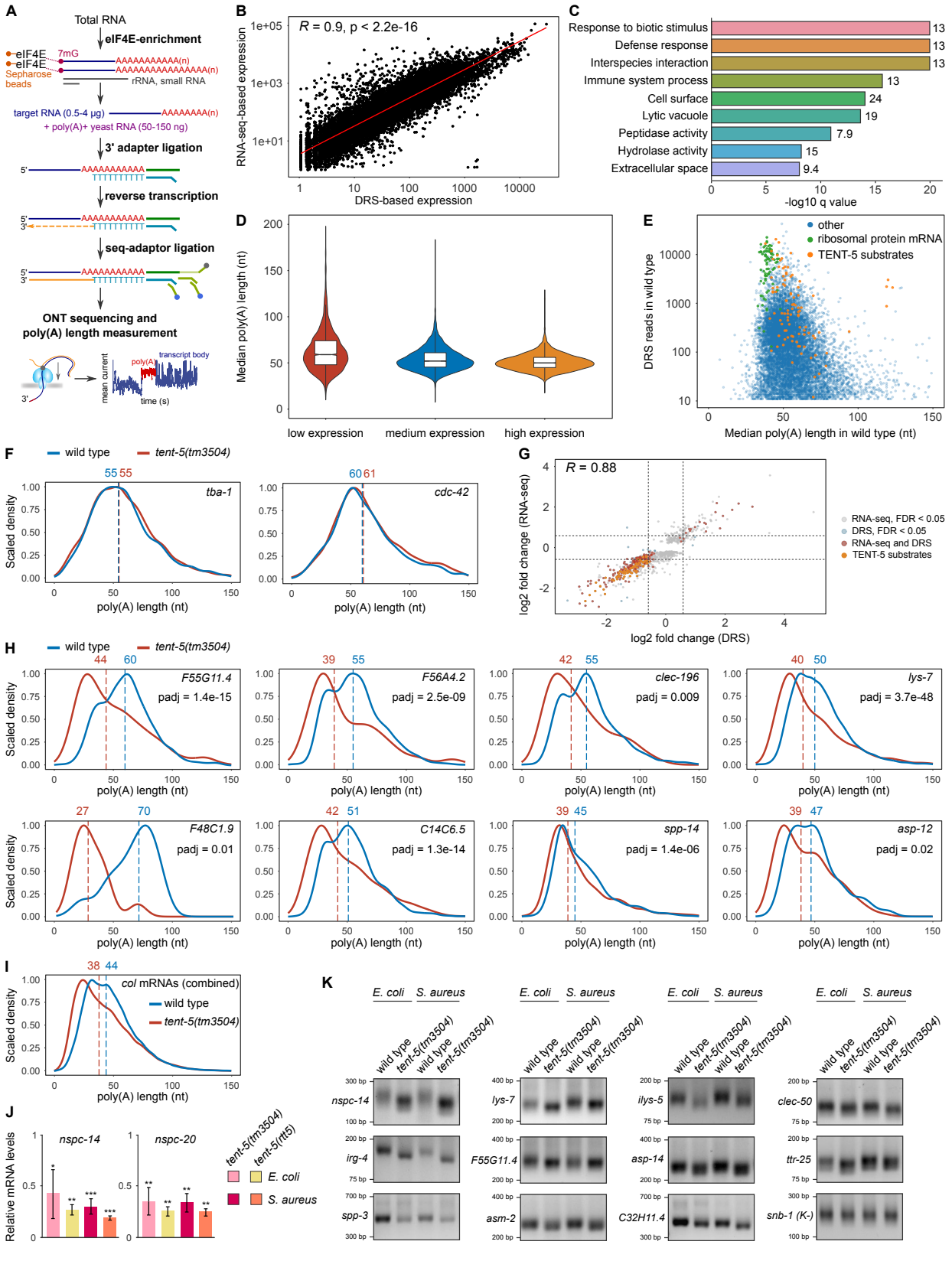
A
Total RNA
eIF4E-enrichment
eIF4E
eIF4E
7mG
Sepharose beads
AAAAAAAAAA(n)
AAAAAAAAAAAAAAAA(n)
rRNA, small RNA
target RNA (0.5-4 µg)
AAAAAAAA(n)
+ poly(A)+ yeast RNA (50-150 ng)
3' adapter ligation
reverse transcription
seq-adaptor ligation
ONT sequencing and
poly(A) length measurement
transcript body
poly(A)
mean current
time (s)
B
R = 0.9, p < 2.2e-16
RNA-seq-based expression
DRS-based expression
C
Response to biotic stimulus
Defense response
Interspecies interaction
Immune system process
Cell surface
Lytic vacuole
Peptidase activity
Hydrolase activity
Extracellular space
-log10 q value
D
Median poly(A) length (nt)
low expression
medium expression
high expression
E
other
ribosomal protein mRNA
TENT-5 substrates
DRS reads in wild type
Median poly(A) length in wild type (nt)
F
wild type
tent-5(tm3504)
tba-1
cdc-42
Scaled density
poly(A) length (nt)
G
R = 0.88
log2 fold change (RNA-seq)
log2 fold change (DRS)
RNA-seq, FDR < 0.05
DRS, FDR < 0.05
RNA-seq and DRS
TENT-5 substrates
H
F55G11.4
padj = 1.4e-15
F56A4.2
padj = 2.5e-09
clec-196
padj = 0.009
lys-7
padj = 3.7e-48
F48C1.9
padj = 0.01
C14C6.5
padj = 1.3e-14
spp-14
padj = 1.4e-06
asp-12
padj = 0.02
I
col mRNAs (combined)
J
nspc-14
nspc-20
Relative mRNA levels
tent-5(tm3504)
tent-5(rt5)
E. coli
S. aureus
K
E. coli
S. aureus
wild type
tent-5(tm3504)
nspc-14
lys-7
ilys-5
clec-50
irg-4
F55G11.4
asp-14
ttr-25
spp-3
asm-2
C32H11.4
snb-1 (K-)

Fig. S5. Transcripts downregulated in the *tent-5*-deficient mutants are the direct targets for polyadenylation by TENT-5. (**A**) Schematic of library preparation for Direct RNA sequencing. (**B**) Correlation between gene expression levels in the wild-type worms measured by DRS and RNA-seq. The red line represents a linear regression line. Genes with normalized expression of minimum 1 were included in the analysis (n=13,632). Values of Pearson's correlation coefficient and statistical test are indicated on the plot. (**C**) Overrepresented functional GO terms of transcripts significantly downregulated (log2FC < -log2(1.5)) in *tent-5(tm3504)* mutant in comparison to the wild-type worms. Numbers on the right indicate the enrichment fold change for each term. (**D**) Violin plots showing the median poly(A) tail length distribution for genes with low (first quartile), medium (interquartile range) and highly (third quartile) expressed mRNA in the wild-type worms. (**E**) Plot illustrating the relationship between median poly(A) tail length and mRNA expression in wild-type worms. TENT-5 substrates are indicated in orange, mRNAs that encode ribosomal proteins are marked in green. (**F-I**) DRS-based poly(A) length profiling of mRNAs that encode established reference genes (**F**), indicated innate immune effectors (**H**) and collagens (**I**). Shown are density distribution plots scaled to 1. Vertical dashed lines represent median poly(A) lengths (nt); padj values (Wilcoxon test) are shown on the top right corner below the mRNA ID. (**G**) Scatter plot illustrates a comparison of the differential expression of genes (FDR < 0.05) between *tent-5* mutant and wild-type worms, as identified by RNA-seq and DRS. Red dots indicate genes differentially expressed in wild-type and mutant worms according to both sequencing methods (n=231), orange dots present TENT-5 substrates (n=96). Dashed lines mark the threshold of the log2(1.5) fold change. Pearson's correlation test. (**J**) RT-qPCR analysis of relative levels of *nspc-14* and *nspc-20* mRNA expression in two *tent-5*-deficient worm strains grown on *E. coli* or exposed to *S. aureus* for 8 hours. Relative abundance of mRNAs was normalized to *act-1* and wild type. Data represent mean ± SD of three biological replicates; $*P \leq 0.05$; $**P \leq 0.01$; $***P \leq 0.001$ (two-tailed t-test). (**K**) Poly(A) tail PCR tests of selected TENT-5-regulated transcripts. Samples were prepared from *tent-5(tm3504)* mutant and wild-type worms infected with *S. aureus* for 8 hours or grown on control *E. coli.* PCR products were analyzed on 2% agarose gels.

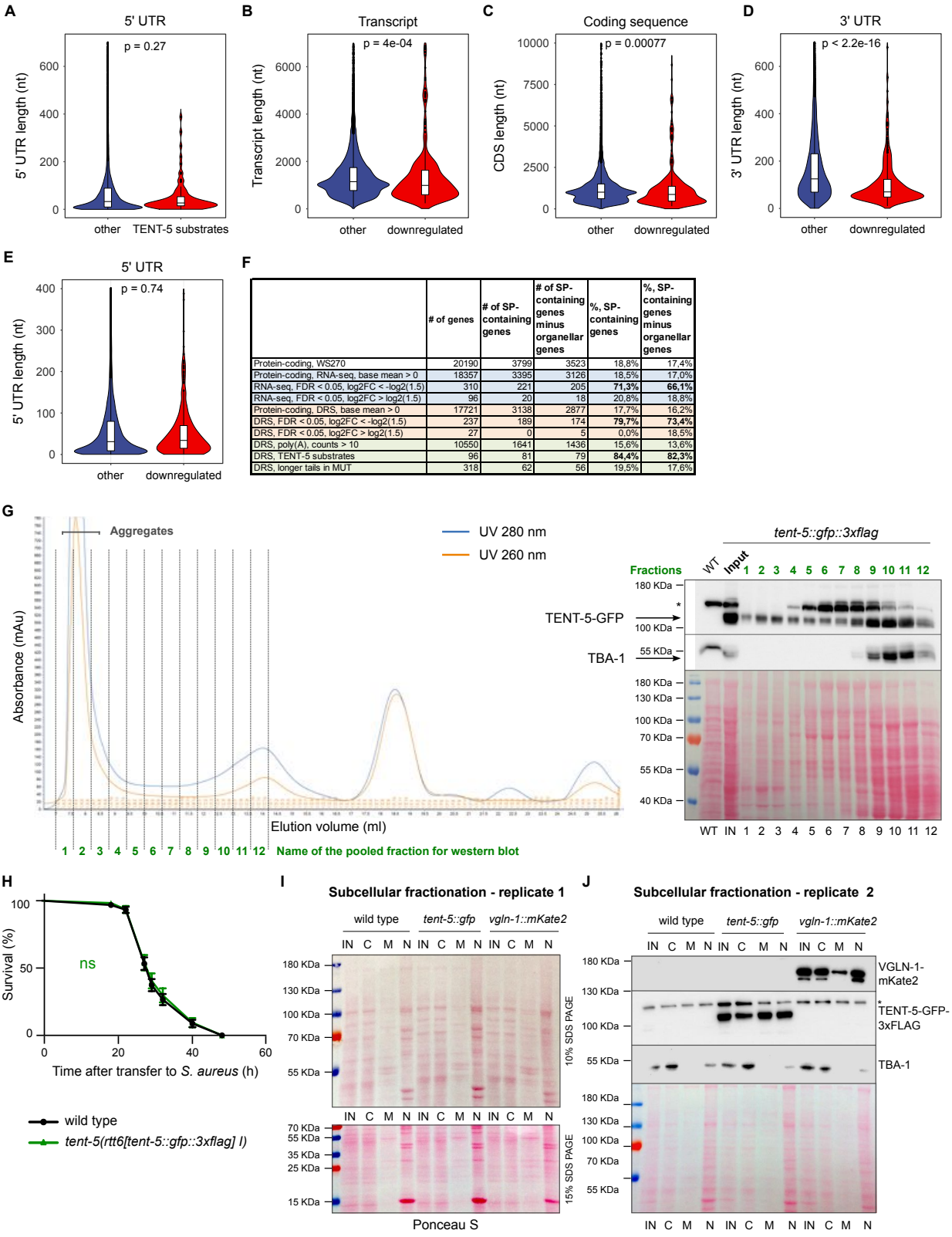

	# of genes	# of SP-containing genes	# of SP-containing genes minus organellar genes	%, SP-containing genes	%, SP-containing genes minus organellar genes
Protein-coding, WS270	20190	3799	3523	18,8%	17,4%
Protein-coding, RNA-seq, base mean > 0	18357	3395	3126	18,5%	17,0%
RNA-seq, FDR < 0.05, log2FC < -log2(1.5)	310	221	205	**71,3%**	**66,1%**
RNA-seq, FDR < 0.05, log2FC > log2(1.5)	96	20	18	20,8%	18,8%
Protein-coding, DRS, base mean > 0	17721	3138	2877	17,7%	16,2%
DRS, FDR < 0.05, log2FC < -log2(1.5)	237	189	174	**79,7%**	**73,4%**
DRS, FDR < 0.05, log2FC > log2(1.5)	27	0	5	0,0%	18,5%
DRS, poly(A), counts > 10	10550	1641	1436	15,6%	13,6%
DRS, TENT-5 substrates	96	81	79	**84,4%**	**82,3%**
DRS, longer tails in MUT	318	62	56	19,5%	17,6%

Fig. S6. TENT-5 regulates mRNAs that encode secreted proteins. (**A**) Violin plot showing length distribution of 5′ UTRs of TENT-5 substrates (n=96) compared to other transcripts

identified by DRS (n=16,568); (p value, Wilcoxon test). Violin plots illustrating length distribution of transcripts (**B**), coding sequences (**C**), 3′ UTRs (D), and 5′ UTRs (**E**) of transcripts, whose expression levels were decreased at least 1.5-fold in *tent-5(tm3504)* mutant worms (n=308) compared to other transcripts identified by RNA-seq (n=18,229); (p value, Wilcoxon test). (**F**) Fractions of genes that encode secreted proteins (%) as defined by (*60*) across indicated datasets. For more details also see data S4. (**G**) The chromatography analysis of total protein extracts from the *tent-5(rtt6)* worms on Superdex 200 (on the left) followed by western blot analysis (on the right). Fractions pooled for western blot analysis are indicated with dotted lines and numbered in green. Most of TENT-5-GFP is present in the fraction corresponding to the TENT-5-GFP molecular weight (pooled fractions 9-11) and a small amount of TENT-5 can be found in macromolecular complexes or aggregates (pooled fractions 1-3). Anti-tubulin (TBA-1) antibodies were used as control, and Ponceau S staining illustrates the relative amount of protein in each pooled fraction. (**H**) Survival of wild-type and *tent-5::gfp::3xflag* worms infected with *S. aureus*; ns – not significant (Log-Rank test). (**I-J**) Subcellular fractionation of proteins isolated from wild-type, *tent-5::gfp::3xflag,* and *vgln-1::mKate2:::3xmyc* strains. (**I**) Ponceau S staining of the whole membrane used for the western blot presented in Fig. 6F (10% SDS PAGE) and membrane containing the same extracts resolved on the 15% SDS PAGE indicating successful fractionation of proteins. (**J**) Second biological replicate of subcellular fractionation shown in Fig. 6F. Anti-tubulin (TBA-1) and anti-RFP (VGLN-1-mKate2) antibodies and Ponceau S staining were used as fractionation controls. IN – input sample, C – cytoplasmic fraction, M – membrane fraction, N – nuclear fraction. Asterisks indicate nonspecific bands.

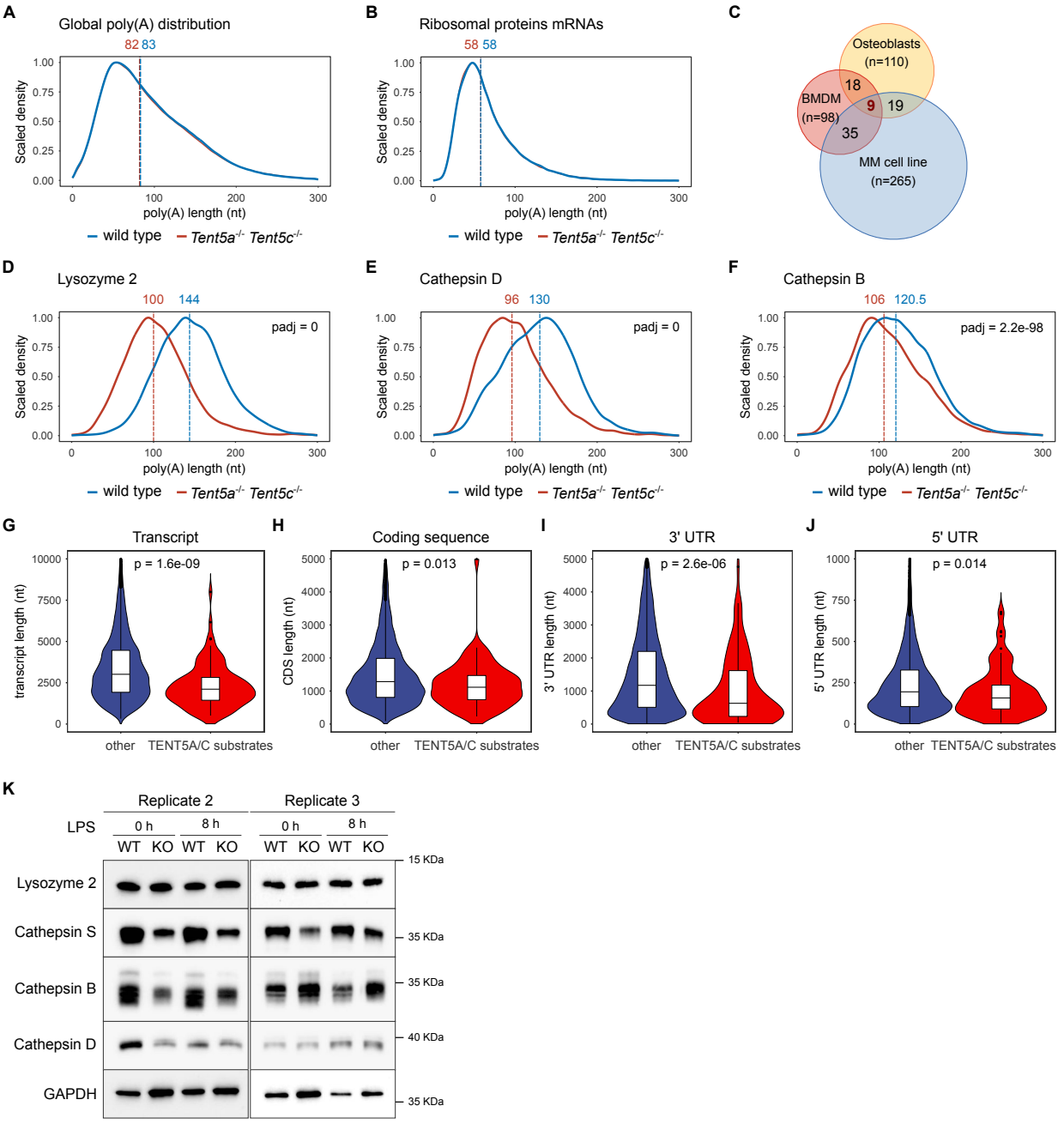

Fig. S7. The role of TENT-5 in innate immunity is evolutionarily conserved. DRS-based poly(A) length profiling of mRNA isolated from *Tent5a*$^{-/-}$ *Tent5c*$^{-/-}$ and wild-type BMDM. Shown are density distribution plots for all transcripts (**A**), mRNAs encoding ribosomal proteins (**B**), *Lyz2* (**D**), *Ctsd* (**E**), and *Ctsb* (**F**) mRNAs scaled to 1. Vertical dashed lines represent median poly(A) lengths (nt); for *Lyz2*, *Ctsd*, and *Ctsb* transcripts padj values (Wilcoxon test) are shown. (**C**) Overlap between TENT5A/C molecular substrates identified in BMDM (red, DRS; this study), osteoblasts (yellow, DRS) (*26*), and multiple myeloma cell lines (blue, RNA-seq after RNA poly(A) length fractionation) (*21*). (**G-I**) Violin plots showing length distribution of transcripts (**G**), coding sequences (**H**), 3′ UTRs (**I**), and 5′ UTRs (**J**) of TENT5A/C substrates (n=98) compared to all other transcripts identified by DRS (n=25,678); (p value, Wilcoxon test).

(**K**) Western blots showing that the lack of TENT5A and TENT5C leads to the lower abundance of LYZ2, CTSS, CTSD, and CTSB both in unstimulated (LPS, 0 hours) and stimulated (LPS, 8 hours) BMDM derived from mutant compared to the wild-type mouse. GAPDH serves as a loading control. Shown are replicates 2 and 3.

Table S1. Survival statistics related to lifespan and pathogenesis assays.

MS: median survival
N: total number of animals that died
P value: compared to the wild type, based on Log-rank (Mantel-Cox) test

	Replicate 1			Replicate 2			Replicate 3		
	MS, days	**N**	**p value**	**MS, days**	**N**	**p value**	**MS, days**	**N**	**p value**
***E. coli HB101*, 20°C, FUdR (Fig. 4A)**									
wild type	26	80		28	91				
tent-5(tm3504)	19	97	p < 0.0001	26	84	0.0091			
tent-5(rtt5)	26	82	ns	28	110	ns			
***E. coli HB101*, 25°C, FUdR (Fig. 4B)**									
wild type	12	151		11	179		14	104	
tent-5(tm3504)	10	129	0.0042	10	176	p < 0.0001	12	113	p < 0.0001
tent-5(rtt5)	12	131	ns	10	184	p < 0.0001	12	138	p < 0.0001
***E. coli HB101* alive, 25°C, FUdR, control to UV-killed HB101 (Fig. S4A)**									
wild type	12	132							
tent-5(tm3504)	11	115	p < 0.0001						
tent-5(rtt5)	10	138	p < 0.0001						
***E. coli HB101* UV-killed, 25°C, FUdR (Fig. S4A)**									
wild type	13	134							
tent-5(tm3504)	13	95	ns						
tent-5(rtt5)	12	130	0,001						
***E. coli HB101* alive, 25°C, FUdR, control to heat-killed HB101 (Fig. S4B)**									
wild type	11	113							
tent-5(tm3504)	11	139	p < 0.0001						
tent-5(rtt5)	10	149	p < 0.0001						
***E. coli* HB101 heat-killed, 25°C, FUdR (Fig. S4B)**									
wild type	13	154							
tent-5(tm3504)	13	144	ns						
tent-5(rtt5)	13	107	ns						
***E. coli OP50* alive, 25°C, FUdR, control to heat-killed HB101 (Fig. S4C-D)**									
wild type	13	170		10	120				
tent-5(tm3504)	12	144	p < 0.0001	9	143	0,0004			
tent-5(rtt5)	12	104	ns	8	126	p < 0.0001			
***E. coli OP50* heat-killed, 25°C, FUdR (Fig. S4C-D)**									
wild type	12	100		14	177				
tent-5(tm3504)	11	130	ns	14	146	ns			
tent-5(rtt5)	11	138	0,0414	14	161	ns			
***S. aureus* (Fig. 4D)**									
wild type	40	75		40	86		38	103	
tent-5(tm3504)	36	111	p < 0.0001	40	107	p < 0.0001	31	144	0.0002
tent-5(rtt5)	36	104	p < 0.0001	40	109	p < 0.0001	31	127	0.0010

***P. aeruginosa PAO1* (Fig. 4E)**									
wild type	7	102		6	132		6	95	
tent-5(tm3504)	6	110	$p < 0.0001$	5	142	$p < 0.0001$	5	90	$p < 0.0001$
tent-5(rtt5)	5	94	$p < 0.0001$	5	161	$p < 0.0001$	5	97	$p < 0.0001$
***E. coli OP50*, 25°C (Fig. S4E)**									
wild type	13	92		12	101				
tent-5(tm3504)	8	127	$p < 0.0001$	10	116	$p < 0.0001$			
***S. marcescens Db10*, 25°C (Fig. S4F)**									
wild type	6	115		4	84				
tent-5(tm3504)	4	173	$p < 0.0001$	3	121	$p < 0.0001$			
***P. luminescens*, 25°C (Fig. S4G)**									
wild type	6	90		4	96				
tent-5(tm3504)	4	103	$p < 0.0001$	3	112	$p < 0.0001$			

Table S2. List of oligonucleotides and sgRNAs used in this study.

ID	Name	Sequence 5′ to 3′	Description
Primers used for PCR genotyping and sequencing of *C. elegans* strains (this study)			
VL001	tent-5-wt-Rev	tcaggtttccactgacaatg	Used for: *tent-5(tm3504), tent-5(rtt5), tent-5(rtt6),* ADZ47
VL002	tent-5-ko-Rev	tgatctcgacctgatattcc	
VL003	tent-5-Fw	gttcacactcgtccaactc	
VL318	tent-5-crispr-Fw	gatcgtgtcgcattccagg	
VL319	tent-5-crispr-Rev	gtgccgacaaattgatggtg	
VL340	tent-5-crispr-Fw2	acgtaagatctccgatccactaattcaaaatttac	
VL355	tent-5-crispr-Fw3	ggtcttcatctggatcagatac	Used for *tent-5(rtt6)*, ADZ47
VL356	tent-5-crispr-Fw4	caaggtaagtttaaacagttc	
VL357	tent-5-crispr-Rev2	ctttaaaatttcagattttgatgta	
Primers used for cloning (this study)			
VL342	sgRNA-universal-Fw	aagcatgcaatttttgagaaactc	Cloning of pDD162-*sgRNA425* (pVL060)
VL343	sgRNA-universal-Rev	gagtgcaccatatgcggtgtgaa	
VL344	sgRNA425-Rev1	tgtagctgcatctggtggcacaagacatctcgcaatagg	
VL345	sgRNA425-Fw1	tgccaccagatgcagctacagttttagagctagaaatagcaagt	
VL346	sgRNA-universal-seq	cgttttacaacgtcgtgactggg	
VL386	sgRNA-universal-Fw2	ctataatttgtcaacctttttcaaaaaaagcatgcaatttttgagaaactc	
VL387	sgRNA-universal-Rev2	cggcatcagagcagattgtactgagagtgcaccatatgcggtgtgaa	
VL347	tent-5-gfp-5′arm-Rev (silent mutations)	catcgatgctcctgaggctcccgatgctccgatgactggaatccaagttgcagcgtccggcggcaagtaga	Cloning of pDD282-*tent-5::gfp::3xflag* (pVL062)
VL348	tent-5-gfp-5′arm-Fw	acgttgtaaaacgacggccagtcgccggcatatgtcgttgaacatgattgatcgtgtcgc	
VL349	tent-5-gfp-3′arm-Fw	cgtgattacaaggatgacgatgacaagagatgatccaattgaacctcttccccctcttac	
VL350	tent-5-gfp-3′arm-Rev	ggaaacagctatgaccatgttatcgatttccagattttgatgtataaacttcgtaggaaatatacag	
VL364	sgRNA-456-F	cgttctttaccaacgacgaggttttagagctagaaatagcaagt	Cloning of pDD162-*sgRNA456* (pVL069)
VL365	sgRNA-456-R	ctcgtcgttggtaaagaacgcaagacatctcgcaatagg	
VL366	vgln-1-mKate2-5arm-R	tatgaccatgattacgccaagctattaaaactccgaactatgatgac	Cloning of pDD287-*vgln-1::mKate2::3xmyc* (pVL070)
VL367	vgln-1-mKate2-5arm-F	catcgatgctcctgaggctcccgatgctccccaacgacgagaggatccccaagca	
VL368	vgln-1-mKate2-3arm-F	ctcgagcagaagttgatcagcgaggaagacttgtaaagaacgttcgaatctggatgattca	
VL369	vgln-1-mKate2-3arm-R	ggaaacagctatgaccatgttatcgatttctctcacatgtacatttagcctacatc	
21	NHATENT-5-Fw	ctagagtcgacatgcgtggaagacgttcccg	Cloning of pCI-*NHA-tent-5*
23	NHATENT-5-Rev	gggaagcggccgctcagatgactggaatccatg	
Primers for RT-qPCR analysis (this study)			
VL031	q-tent-5-Fw	ggcaacttcccaacaatctcc	Efficiency: 1.93
VL032	q-tent-5-Rev	gaagaggctacaaatgatgcgg	
VL453	q-tent-5-Fw2	gtgctcccgcttcttcatcg	2.0
VL454	q-tent-5-Rev2	ccattgatcgtaagtggctccg	
VL033	q-act-1-Fw	gctggacgtgatcttactgattacc	1.95

VL034	q-act-1-Rev	gtagcagagcttctccttgatgtc	
VL096	q-ilys-5-Fw	tgcctggaagagatgtgctg	1.96
VL097	q-ilys-5-Rev	tgcactgagacttgtagcgg	
VL101	q-spp-14-Fw	gaccaccttctgccttctgg	2.0
VL102	q-spp-14-Rev	gcattgtcctgttggcttgg	
VL104	q-spp-3-Fw	gtcgacgctgaatgcaagaag	1.93
VL105	q-spp-3-Rev	ttgggtcgagcttggtgtc	
VL108	q-clec-160-Fw	ggcagcaatgcagtatggac	2.0
VL109	q-clec-160-Rev	acgctcgtctagaaatcggac	
VL111	q-clec-50-Fw	accgattccaactacctgcc	1.98
VL112	q-clec-50-Rev	tccatccttggtcgcaagac	
VL116	q-irg-4-Fw	tcggtcgaaacccaattccc	1.92
VL117	q-irg-4-Rev	aaattggatcgacgcagcac	
VL119	q-F55G11.4-Fw	tgttgcatctattgggcagg	1.92
VL120	q-F55G11.4-Rev	ctcctggtgcagcgtattcc	
VL122	q-irg-5-Fw	tcatggacctgattacaccgc	1.94
VL123	q-irg-5-Rev	agcgaatcggatggagtacg	
VL124	q-asp-14-Fw	ttaccttgacaccaccaccg	1.99
VL125	q-asp-14-Rev	aagggagtcaaacacctggc	
VL130	q-T21H3.1-Fw	ttcggcctttgtgctaccag	1.98
VL131	q-T21H3.1-Rev	tggcgtcgttgtatgggatg	
VL132	q-K12H4.7-Fw	acattcggagaggctcaatctg	1.94
VL133	q-K12H4.7-Rev	tccgaactcagtgcaagtctg	
VL206	q-nspc-14-Fw	gccctctgccttgtttctgc	1.94
VL207	q-nspc-14-Rev	aagattcgccaccattgacacc	
VL208	q-nspc-20-Fw	tgtgtgcataactgtgctgctg	1.90
VL209	q-nspc-20-Rev	gcttctttgctgggaatgttgc	
VL224	q-spp-5-Fw	ccgataaggatgccaatgtc	1.98
VL225	q-spp-5-Rev	gggtctaccttgctgttgac	
VL231	q-lys-7-Fw	atccggtcgtgatctgattc	2.0
VL232	q-lys-7-Rev	gattgttgactcatcccttc	
VL236	q-C14C6.5-Fw	tggtgtcagtgactgcccag	2.0
VL237	q-C14C6.5-Rev	agccacagtatccgcaggtc	
VL406	q-F28B4.3-Fw1	agaccatctctggtggaagcg	1.96
VL407	q-F28B4.3-Rev	tcctccattggtgctagcgg	
VL409	qr-ttr-45-Fw1	gcttgtggctgcaatgaggg	1.98
VL410	q-ttr-45-Rev	ccgagtcctcttcccagagc	
VL414	q-ZK1320.2-Fw	aatgccggatggaacctggg	1.96
VL415	q-ZK1320.2-Rev	acatctgcactgttagttgtggg	
Primers used for Poly(A) PCR tests (this study)			
	RA3-15N	/5rApp/ctgacnnnnnnnnnnnnnnnntggaattctcgg gtgccaagg/3ddC/ (5′ pre-adenylated, with 15 nt unique molecular identifier)	3′ adaptor
	RPI	caagcagaagacggcatacgagatnnnnnngtgactgga gttccttggcacccgagaattcca	RNA PCR Rev Primer
VL294	RP-uni-Rev	caagcagaagacggcatacgagat	
VL116	r-irg-4-Fw1	tcggtcgaaacccaattccc	
VL446	r-irg-4-Fw2	gacaaacatcactcgtccatcg	
VL156	r-lys-7-Fw1	actcctgccaacttcaatgact	

VL235	r-lys-7-Fw2	aatgatacggcgaccaccgagatctacacgttcagagttcta cagtccgacgatcatgctggaggatttgtgcaaggaa	
VL212	r-clec-50-Fw1	ggatctcgcgtggatcggta	
VL213	r-clec-50-Fw2	aatgatacggcgaccaccgagatctacacgttcagagttcta cagtccgacgatcctgcaagaagggatctattcatgca	
VL164	r-F55G11.4-Fw1	gtgaacgcgggagcacata	
VL211	r-F55G11.4-Fw2	aatgatacggcgaccaccgagatctacacgttcagagttcta cagtccgacgatcgtggcaaggctgtattcacgttta	
VL217	r-nspc-14-Fw1	gagttctgtgctggtgtcaatg	
VL218	r-nspc-14-Fw2	tgtgtatgttgcttcagtcgt	
VL104	r-spp-3-Fw1	gtcgacgctgaatgcaagaag	
VL221	r-spp-3-Fw2	cgtctgcaccaagcttggaatgtg	
VL165	r-asp-14-Fw1	tcagcacaaacgttatgaatgct	
VL216	r-asp-14-Fw2	aatgatacggcgaccaccgagatctacacgttcagagttcta cagtccgacgatccactccagcgcttctccaagattag	
VL214	r-asm-2-Fw1	ctcacctcaatcgtggtccg	
VL215	r-asm-2-Fw2	aatgatacggcgaccaccgagatctacacgttcagagttcta cagtccgacgatcgatcatttaacaaaatagtttcac	
VL222	r-ttr-25-Fw1	cacagatgcaaccacgtcgg	
VL223	r-ttr-25-Fw2	ggagagggtactgattgcattca	
VL268	r-snb-1-Fw1	cggcgcgataagctgcgtga	
VL269	r-snb-1-Fw2	cagactaacaacatgccttctc	
VL449	r-C32H11.4-Fw1	cggatctgaaactgcgttcg	
VL450	r-C32H11.4-Fw2	cactcacgttctacggcgaa	
VL096	r-ilys-5-Fw1	tgcctggaagagatgtgctg	
VL475	r-ilys-5-Fw2	ggatactatgaagactgcgg	
Primers for RL northern blot probe preparation (this study)			
	RL_Fw	atgattactggtccacaatgg	
	RL_Rev	ggacacgctcaacaaacgat	
Oligonucleotides used to generate *tent-5(rtt5)* strain by CRISPR/Cas9			
VL311	tracrRNA-fragment	AAAAAGCACCGACTCGGTGCCACTTT TTCAAGTTGATAACGGACTAgccttattttaa cttgctatttctagctcta	
VL312	crRNA01-tent-5	gaaattaatacgactcactatagggGTTCAATTGGA TCAGATGACgttttagagctagaaatagcaagttaaaa taaggc	Description: underlined – T7 RNA promoter; blue – 5′N20 guide RNA sequence; red – crRNA scaffold
VL315	crRNA02-tent-5	gaaattaatacgactcactatagggCTCATTCTGTT TGTTCCGTGgttttagagctagaaatagcaagttaaaa taaggc	
VL313	crRNA-dpy-10	gaaattaatacgactcactatagggGCTACCATAGG CACCACGAGgttttagagctagaaatagcaagttaaa ataaggc	
VL314	ssODN-dpy-10	cacttgaacttcaatacggcaagatgagaatgactggaaacc gtaccgcatgcggtgcctatggtagcggagcttcacatggctt cagaccaacagcctat	(*94*)
VL326	ssODN-tent-5	ctggattttaaattattaatttaaaaaaaaattttcagttggctcat catggaacaaacagatccaattgaacctcttccccctcttacat tctgtccacccttcttcgaaaatcaaaccac	upstream of the start, down-stream of the stop codon of *tent-5* (d)

Primers for genotyping of the previously published mouse lines (with reference)			
	Tent5c KO-Fw	aggtcctgactgaggtcgtg	(*21*)
	Tent5c KO-Rev	ttcctcaaaatccccgtaca	
	Tent5a-3xFLAG-Fw	tggtaaacgagagtacggtg	(*26*)
	Tent5a-3xFLAG-Rev	ctggctgctttttaccaaca	
	Tent5c-3xFLAG-Fw	gaccctgaacctcatctctc	(*21*)
	Tent5c-3xFLAG-Rev	tatgggtccttttagggttg	
sgRNAs, ssDNA and primers used for *Tent5a*$^{Flox/Flox}$ cKO mouse line			
	sgRNA_LoxP_left	tatgggcgtcacgatcggggagg	guide RNA sequence
	sgRNA_LoxP_right	actaatgcgcgtgagtggtgtgg	
	ssDNA donor	GCTGGGCATTGGGGTCGGTGAGGGTTGGG GGAGGAGGGCTACTATGGGCGTCACGATC GGATAACTTCGTATAGCATACATTATACG AAGTTATGGatccAGGGGAAGCCCAGGCCC CTcggcgggaccctgtcccctcacccgcacacctctctgccgct cccctaaatccactctttcctcttagGACTGACCAAGGCC AAGTGGCTTTCGGAGGGCACTACATGGCC GAGGGCGAAGGGTACTTTGCCATGGCAG AGGACGAGCTGACCGGCGGCCCTTACATC CCCCTGGGTGGTGACTTCGGCGGCGGCGG CAGCAGCTTCGGCGACCGCTGCTCGGACT ATTGCGAAAGCCCCACGGCGCACTGCAAT GTGCTGAACTGGGAGCAAGTGCAGCGGTT GGACGGCATTCTGAGCGAGACCATCCCGA TCCACGGGCGCGGCAACTTCCCCACGCTC GAGCTGCAGCCAAGCCTGATTGTGAAGGT GGTGAGGAGGCGCCTGGAAGAGAAGGGC ATAGGTGTCCGCGACGTGCGCCTCAACGG CTCAGCCGCCAGTCACGTCCTGCACCAGG ACAGTGGCCTAGGCTACAAGGACCTGGAC CTCATCTTCTGCGCTGACCTGCGTGGGGA AGAGGAGTTTCAGACTGTGAAGGACGTCG TTCTGGATTGCCTGTTAGACTTCTTGCCCG AAGGGGTGAACAAGGAGAAGATCACACC GCTCACTCTCAAGgtaaagccacctgatgggcttgggca gagcaggggtggggagaaagcaagcccagcttgccttgactgccg tcagtatggccatagtgagttcgtttatttatttttttattatttttttttcacg agcgcaCTAATGCGCGTGAGTGGatccATAAC TTCGTATAGCATACATTATACGAAGTTAT TGTGGAGTGTTTTAGTTTCCTGGGAGATC CAGCGCCACAACTCTGTGCTTCCTCCTCTG CGTTTC	Description: *LoxP* sites are underlined, BamHI sites are highlighted in grey
	Tent5a_cKO_sFw	actctcgcttgtgctttcca	sequencing
	Tent5a_cKO_sRv	tcagttctgcttcaggctgc	
	Tent5a_cKO_gFw	caagcctgattgtgaaggtg	Mice genotyping
	Tent5a_cKO_gRv	aaggaagagaaggaaacgca	
	For genotyping of *Tent5a* cKO mice, PCR products generated with Tent5a_cKO_gFw/gRv primers were digested with BamHI: • WT: undigested 489 bp, digested 489 bp • cKO: undigested 527 bp, digested: 117 bp		
	A_FloX_F1	actctcgcttgtgctttcca	BMDM genotyping
	A_FloX_F2	tcagactgtgaaggacgtcg	
	A_FloX_R1	tcagttctgcttcaggctgc	

Table S3. List of DNA constructs used in this study.

pDNA	Source	Reference
pCFJ90-*Pmyo-2::mCherry::unc-54utr*	Dr. J. J. Ewbank	Addgene plasmid # 19327; see ref. (*119*)
pCFJ104-*Pmyo-3::mCherry::unc-54utr*	Dr. J. J. Ewbank	Addgene Plasmid # 19328; see ref. (*119*)
pCFJ151	Dr. J. J. Ewbank	Addgene Plasmid # 19330; see ref. (*119*)
pDD162 (*Peft-3::Cas9* + Empty sgRNA)	Dr. B. Goldstein	Addgene Plasmid # 47549; see ref. (*120*)
pDD282	Dr. B. Goldstein	Addgene Plasmid # 66823; see ref. (*120*)
pDD287	Dr. B. Goldstein	Addgene Plasmid # 70685; see ref. (*120*)
pRH269-*Pmyo-2::GFP::unc-54utr*	Dr. K. Drabikowski	
pCIneo-NHA	Dr. Witold Filipowicz	see ref. (*104*)
pRL-5BoxB	Dr. Witold Filipowicz	see ref. (*104*)
pMD2.G	Dr. Didier Trono	Addgene Plasmid # 12259
psPAX2	Dr. Didier Trono	Addgene Plasmid # 12260
pCAG-Cre-IRES2-GFP	Dr. Jacek Jaworski	Addgene Plasmid # 26646; see ref. (*121*)
pCIneo-*NHA-tent-5*^{WT}	This work	
pCIneo-*NHA-tent-5*^{MUT} (MUT = D151A, D153A in *tent-5* isoform a)	This work	
pDD162-*sgRNA425* (pVL060)	This work	
pDD162-*sgRNA456* (pVL069)	This work	
pDD282-*tent-5::gfp::3xflag* (pVL062)	This work	
pDD287-*vgln-1::mKate2::3xmyc* (pVL070)	This work	

Table S4. Protein sequences used for the phylogenetic analysis.

Organism	Protein	WormBase or UniProt ID
Caenorhabditis elegans		
	TENT-5	F55A12.9.d1
	GLD-2	ZC308.1c.1
	GLD-4	ZK858.1
	USIP-1	ZK863.4
	PUP-1/CID-1	K10D2.3
	PUP-2	K10D2.2
	PUP-3	F59A3.9
	MUT-2	K04F10.6b.1
Homo sapiens		
	TENT5A	Q96IP4
	TENT5B	Q96A09
	TENT5C	Q5VWP2
	TENT5D	Q8NEK8
	TENT2	Q6DFA8
	TENT4A	Q5XG87
	TENT4B	Q8NDF8
	TENT6	Q9NVV4
	TENT1	Q9H6E5
	TUT4	Q5TAX3
	TUT7	Q5VYS8
Mus musculus		
	TENT5A	A0A087WS27
	TENT5B	Q8C152
	TENT5C	Q5SSF7
	TENT5D	B1ATX6
	TENT2	Q91YI6
	TENT4A	Q6PB75
	TENT4B	Q68ED3
	TENT6	Q9D0D3
	TENT1	Q8R3F9
	TUT4	B2RX14
	TUT7	Q5BLK4
Xenopus laevis		
	TENT2-a	Q641A1
	TENT2-b	Q6DFA8
	TENT4B	A0A1L8GKF9
	TUT4	A0A1L8GMG3
	TUT7	A0A1L8HZ12
	TENT5A	Q08AY7
	TENT5B	Q66J95
	TENT5D	A0A1L8F355

Data S1. (separate file)
Differential expression of genes in age-synchronized L4-staged *tent-5(tm3504)* mutant worms compared to wild type grown on *E. coli* HB101 at 25°C (RNA-seq, DESeq2 results).

Data S2. (separate file)
Proteins abundance in age-synchronized L4-staged *tent-5(tm3504)* mutant compared to wild type worms grown on *E. coli* HB101 at 20°C (Mass Spectrometry).

Data S3. (separate file)
Differential expression of genes in *tent-5(tm3504)* mutant worms compared to wild type infected with *S. aureus* for 8h at 25°C (RNA-seq, DESeq2 results).

Data S4. (separate file)
Differential adenylation analysis on data from Direct RNA sequencing of RNA isolated from age-synchronized L4-staged *tent-5(tm3504)* and wild-type worms grown on *E. coli* HB101 at 25°C (DRS).

Data S5. (separate file)
Differential expression of genes in age-synchronized L4-staged *tent-5(tm3504)* mutant compared to wild-type worms grown on *E. coli* HB101 at 25°C (DRS, DESeq2 results).

Data S6. (separate file)
Differential adenylation and gene expression analyses on data from Direct RNA sequencing of RNA isolated from BMDM of *Tent5a*$^{Flox/Flox}$ *Tent5c*$^{-/-}$ and wild-type mice (DRS).

REFERENCES AND NOTES

1. J. A. Hoffmann, F. C. Kafatos, C. A. Janeway, R. A. B. Ezekowitz, Phylogenetic perspectives in innate immunity. *Science* **284**, 1313–1318 (1999).

2. A. Iwasaki, R. Medzhitov, Control of adaptive immunity by the innate immune system. *Nat. Immunol.* **16**, 343–353 (2015).

3. K. Buchmann, Evolution of innate immunity: Clues from invertebrates via fish to mammals. *Front. Immunol.* **5**, 1–8 (2014).

4. D. H. Kim, J. J. Ewbank, Signaling in the innate immune response. *WormBook* **2018**, 1–35 (2018).

5. J. E. Irazoqui, J. M. Urbach, F. M. Ausubel, Evolution of host innate defence: Insights from *Caenorhabditis elegans* and primitive invertebrates. *Nat. Rev. Immunol.* **10**, 47–58 (2010).

6. G. Gasteiger, A. D'osualdo, D. A. Schubert, A. Weber, E. M. Bruscia, D. Hartl, Cellular innate immunity: An old game with new players. *J. Innate Immun.* **9**, 111–125 (2017).

7. S. Carpenter, E. P. Ricci, B. C. Mercier, M. J. Moore, K. A. Fitzgerald, Post-transcriptional regulation of gene expression in innate immunity. *Nat. Rev. Immunol.* **14**, 361–376 (2014).

8. Y. Shi, J. L. Manley, The end of the message: Multiple protein–RNA interactions define the mRNA polyadenylation site. *Genes Dev.* **29**, 889–897 (2015).

9. J. Neve, R. Patel, Z. Wang, A. Louey, A. M. Furger, Cleavage and polyadenylation: Ending the message expands gene regulation. *RNA Biol.* **14**, 865–890 (2017).

10. A. L. Jalkanen, S. J. Coleman, J. Wilusz, Determinants and implications of mRNA poly(A) tail size—Does this protein make my tail look big? *Semin. Cell Dev. Biol.* **34**, 24–32 (2014).

11. Y. Bin Yan, Deadenylation: Enzymes, regulation, and functional implications. *Wiley Interdiscip. Rev. RNA* **5**, 421–443 (2014).

12. G. Martin, W. Keller, RNA-specific ribonucleotidyl transferases. *RNA* **13**, 1834–1849 (2007).

13. S. Yu, V. N. Kim, A tale of non-canonical tails: Gene regulation by post-transcriptional RNA tailing. *Nat. Rev. Mol. Cell Biol.* **21**, 542–556 (2020).

14. V. Liudkovska, A. Dziembowski, Functions and mechanisms of RNA tailing by metazoan terminal nucleotidyltransferases. *Wiley Interdiscip. Rev. RNA* **12**, e1622 (2021).

15. J. H. Kim, J. D. Richter, Opposing polymerase-deadenylase activities regulate cytoplasmic polyadenylation. *Mol. Cell* **24**, 173–183 (2006).

16. K. W. Kim, T. L. Wilson, J. Kimble, GLD-2/RNP-8 cytoplasmic poly(A) polymerase is a broad-spectrum regulator of the oogenesis program. *Proc. Natl. Acad. Sci. U.S.A.* **107**, 17445–17450 (2010).

17. M. Nousch, A. Yeroslaviz, C. R. Eckmann, Stage-specific combinations of opposing poly(A) modifying enzymes guide gene expression during early oogenesis. *Nucleic Acids Res. Res.* **47**, 10881–10893 (2019).

18. E. K. Jae, E. Drier, S. A. Barbee, M. Ramaswami, J. C. P. Yin, M. Wickens, GLD2 poly(A) polymerase is required for long-term memory. *Proc. Natl. Acad. Sci. U.S.A.* **105**, 14644–14649 (2008).

19. T. Udagawa, S. A. Swanger, K. Takeuchi, J. H. Kim, V. Nalavadi, J. Shin, L. J. Lorenz, R. S. Zukin, G. J. Bassell, J. D. Richter, Bidirectional control of mRNA translation and synaptic plasticity by the cytoplasmic polyadenylation complex. *Mol. Cell* **47**, 253–266 (2012).

20. K. Kuchta, A. Muszewska, L. Knizewski, K. Steczkiewicz, L. S. Wyrwicz, K. Pawlowski, L. Rychlewski, K. Ginalski, FAM46 proteins are novel eukaryotic non-canonical poly(A) polymerases. *Nucleic Acids Res.* **44**, 3534–3548 (2016).

21. S. Mroczek, J. Chlebowska, T. M. Kuliński, O. Gewartowska, J. Gruchota, D. Cysewski, V. Liudkovska, E. Borsuk, D. Nowis, A. Dziembowski, The non-canonical poly(A) polymerase *FAM46C* acts as an onco-suppressor in multiple myeloma. *Nat. Commun.* **8**, 619 (2017).

22. Y. X. Zhu, C. X. Shi, L. A. Bruins, P. Jedlowski, X. Wang, K. M. Kortüm, M. Luo, J. M. Ahmann, E. Braggio, A. K. Stewart, Loss of *FAM46C* promotes cell survival in myeloma. *Cancer Res.* **77**, 4317–4327 (2017).

23. A. Bilska, M. Kusio-kobia, P. S. Krawczyk, O. Gewartowska, B. Tarkowski, K. Koby, D. Nowis, J. Golab, J. Gruchota, E. Borsuk, A. Dziembowski, S. Mroczek, Immunoglobulin expression and the humoral immune response is regulated by the non-canonical poly(A) polymerase TENT5C. *Nat. Commun.* **11**, 1–17 (2020).

24. A. B. Herrero, D. Quwaider, L. A. Corchete, M. V. Mateos, R. García-Sanz, N. C. Gutiérrez, FAM46C controls antibody production by the polyadenylation of immunoglobulin mRNAs and inhibits cell migration in multiple myeloma. *J. Cell. Mol. Med.* **00**, 1–12 (2020).

25. J. L. Hu, H. Liang, H. Zhang, M. Z. Yang, W. Sun, P. Zhang, L. Luo, J. X. Feng, H. Bai, F. Liu, T. Zhang, J. Y. Yang, Q. Gao, Y. Long, X. Y. Ma, Y. Chen, Q. Zhong, B. Yu, S. Liao, Y. Wang, Y. Zhao, M. S. Zeng, N. Cao, J. Wang, W. Chen, H. T. Yang, S. Gao, FAM46B is a prokaryotic-like cytoplasmic poly(A) polymerase essential in human embryonic stem cells. *Nucleic Acids Res.* **48**, 2733–2748 (2020).

26. O. Gewartowska, G. Aranaz-Novaliches, P. S. Krawczyk, S. Mroczek, M. Kusio-Kobiałka, B. Tarkowski, F. Spoutil, O. Benada, O. Kofroňová, P. Szwedziak, D. Cysewski, J. Gruchota, M. Szpila, A. Chlebowski, R. Sedlacek, J. Prochazka, A. Dziembowski, Cytoplasmic polyadenylation by TENT5A is required for proper bone formation. *Cell Rep.* **35**, 109015 (2021).

27. J. Coller, M. Wickens, Tethered function assays: An adaptable approach to study RNA regulatory proteins. *Methods Enzymol.* **429**, 299–321 (2007).

28. E. R. Troemel, S. W. Chu, V. Reinke, S. S. Lee, F. M. Ausubel, D. H. Kim, p38 MAPK regulates expression of immune response genes and contributes to longevity in *C. elegans*. *PLOS Genet.* **2**, 1725–1739 (2006).

29. T. Roeder, M. Stanisak, C. Gelhaus, I. Bruchhaus, J. Grötzinger, M. Leippe, Caenopores are antimicrobial peptides in the nematode *Caenorhabditis elegans* instrumental in nutrition and immunity. *Dev. Comp. Immunol.* **34**, 203–209 (2010).

30. H. Schulenburg, M. P. Hoeppner, J. Weiner, E. Bornberg-Bauer, Specificity of the innate immune system and diversity of C-type lectin domain (CTLD) proteins in the nematode *Caenorhabditis elegans*. *Immunobiology* **213**, 237–250 (2008).

31. I. Engelmann, A. Griffon, L. Tichit, F. Montañana-Sanchis, G. Wang, V. Reinke, R. H. Waterston, L. D. W. Hillier, J. J. Ewbank, A comprehensive analysis of gene expression changes provoked by bacterial and fungal infection in *C. elegans*. *PLOS ONE* **6**, e19055 (2011).

32. C. Taffoni, N. Pujol, Mechanisms of innate immunity in *C. elegans* epidermis. *Tissue Barriers* **3**, 1–8 (2015).

33. J. H. Thomas, Concerted evolution of two novel protein families in *Caenorhabditis species*. *Genetics* **172**, 2269–2281 (2006).

34. D. Wong, D. Bazopoulou, N. Pujol, N. Tavernarakis, J. J. Ewbank, Genome-wide investigation reveals pathogen-specific and shared signatures in the response of *Caenorhabditis elegans* to infection. *Genome Biol.* **8**, R194 (2007).

35. G. V. Mallo, C. L. Kurz, C. Couillault, N. Pujol, S. Granjeaud, Y. Kohara, J. J. Ewbank, Inducible antibacterial defense system in *C. elegans*. *Curr. Biol.* **12**, 1209–1214 (2002).

36. C. T. Murphy, S. A. McCarroll, C. I. Bargmann, A. Fraser, R. S. Kamath, J. Ahringer, H. Li, C. Kenyon, Genes that act downstream of DAF-16 to influence the lifespan of *Caenorhabditis elegans*. *Nature* **424**, 277–283 (2003).

37. O. Visvikis, N. Ihuegbu, S. A. Labed, L. G. Luhachack, A. M. F. Alves, A. C. Wollenberg, L. M. Stuart, G. D. Stormo, J. E. Irazoqui, Innate host defense requires TFEB-mediated transcription of cytoprotective and antimicrobial genes. *Immunity* **40**, 896–909 (2014).

38. A. Sinha, R. Rae, I. Iatsenko, R. J. Sommer, System wide analysis of the evolution of innate immunity in the nematode model species *Caenorhabditis elegans* and *Pristionchus pacificus*. *PLOS ONE* **7**, e44255 (2012).

39. S. Alper, S. J. McBride, B. Lackford, J. H. Freedman, D. A. Schwartz, Specificity and complexity of the *Caenorhabditis elegans* innate immune response. *Mol. Cell. Biol.* **27**, 5544–5553 (2007).

40. W. Yang, K. Dierking, P. C. Rosenstiel, H. Schulenburg, GATA transcription factor as a likely key regulator of the *Caenorhabditis elegans* innate immune response against gut pathogens. *Fortschr. Zool.* **119**, 244–253 (2016).

41. E. A. Evans, T. Kawli, M. W. Tan, Pseudomonas aeruginosa suppresses host immunity by activating the DAF-2 insulin-like signaling pathway in *Caenorhabditis elegans*. *PLOS Pathog.* **4**, e1000175 (2008).

42. R. P. Shivers, M. J. Youngman, D. H. Kim, Transcriptional responses to pathogens in *Caenorhabditis elegans*. *Curr. Opin. Microbiol.* **11**, 251–256 (2008).

43. X. X. Lin, I. Sen, G. E. Janssens, X. Zhou, B. R. Fonslow, D. Edgar, N. Stroustrup, P. Swoboda, J. R. Yates, G. Ruvkun, C. G. Riedel, DAF-16/FOXO and HLH-30/TFEB function as combinatorial transcription factors to promote stress resistance and longevity. *Nat. Commun.* **9**, 4400 (2018).

44. D. Gems, D. L. Riddle, Genetic, behavioral and environmental determinants of male longevity in *Caenorhabditis elegans*. *Genetics* **154**, 1597–1610 (2000).

45. D. Garigan, A. L. Hsu, A. G. Fraser, R. S. Kamath, J. Abringet, C. Kenyon, Genetic analysis of tissue aging in *Caenorhabditis elegans*: A role for heat-shock factor and bacterial proliferation. *Genetics* **161**, 1101–1112 (2002).

46. J. E. Irazoqui, E. R. Troemel, R. L. Feinbaum, L. G. Luhachack, B. O. Cezairliyan, F. M. Ausubel, Distinct pathogenesis and host responses during infection of *C. elegans* by *P. aeruginosa* and *S. aureus*. *PLOS Pathog.* **6**, 1–24 (2010).

47. C. L. Kurz, S. Chauvet, E. Andrès, M. Aurouze, I. Vallet, G. P. F. Michel, M. Uh, J. Celli, A. Filloux, S. De Bentzmann, I. Steinmetz, J. A. Hoffmann, B. B. Finlay, J.-P. Gorvel, D. Ferrandon, J. J. Ewbank, Virulence factors of the human opportunistic pathogen *Serratia marcescens* identified by in vivo screening. *EMBO J.* **22**, 1451–1460 (2003).

48. C. Couillault, J. J. Ewbank, Diverse bacteria are pathogens of *Caenorhabditis elegans*. *Infect. Immun.* **70**, 4705–4707 (2002).

49. M. F. Palominos, A. Calixto, Quantification of bacteria residing in *Caenorhabditis elegans* intestine. *Bio Protoc.* **10**, 1–12 (2020).

50. F. Rodriguez Ayala, S. Cogliati, C. Bauman, C. Leñini, M. Bartolini, J. Villalba, F. Argañaraz, R. Grau, Culturing bacteria from *Caenorhabditis elegans* gut to assess colonization proficiency. *Bio Protoc.* **7**, e2345 (2017).

51. M. E. Hoinville, A. C. Wollenberg, Changes in *Caenorhabditis elegans* gene expression following exposure to *Photorhabdus luminescens* strain TT01. *Dev. Comp. Immunol.* **82**, 165–176 (2018).

52. I. Legnini, J. Alles, N. Karaiskos, S. Ayoub, N. Rajewsky, FLAM-seq: Full-length mRNA sequencing reveals principles of poly(A) tail length control. *Nat. Methods* **16**, 879–886 (2019).

53. S. A. Lima, L. B. Chipman, A. L. Nicholson, Y. H. Chen, B. A. Yee, G. W. Yeo, J. Coller, A. E. Pasquinelli, Short poly(A) tails are a conserved feature of highly expressed genes. *Nat. Struct. Mol. Biol.* **24**, 1057–1063 (2017).

54. J. Tao, Y. Hao, X. Li, H. Yin, X. Nie, J. Zhang, B. Xu, Q. Chen, B. Li, Systematic identification of housekeeping genes possibly used as references in *Caenorhabditis elegans* by large-scale data integration. *Cell* **9**, 786 (2020).

55. C. Y. Ewald, J. N. Landis, J. P. Abate, C. T. Murphy, T. K. Blackwell, Dauer-independent insulin/IGF-1-signalling implicates collagen remodelling in longevity. *Nature* **519**, 97–101 (2015).

56. D. Sellegounder, Y. Liu, P. Wibisono, C. H. Chen, D. Leap, J. Sun, Neuronal GPCR NPR-8 regulates *C. elegans* defense against pathogen infection. *Sci. Adv.* **5**, eaaw4717 (2019).

57. Y. Liu, D. Martinez-Martinez, C. L. Essmann, M. R. Cruz, F. Cabreiro, D. A. Garsin, Transcriptome analysis of *Caenorhabditis elegans* lacking heme peroxidase SKPO-1 reveals an altered response to *Enterococcus faecalis*. *G3 (Bethesda)* **11**, jkaa055 (2021).

58. I. Gallotta, A. Sandhu, M. Peters, M. Haslbeck, R. Jung, S. Agilkaya, J. L. Blersch, C. Rödelsperger, W. Röseler, C. Huang, R. J. Sommer, D. C. David, Extracellular proteostasis prevents aggregation during pathogenic attack. *Nature* **584**, 410–414 (2020).

59. T. L. Bailey, DREME: Motif discovery in transcription factor ChIP-seq data. *Bioinformatics* **27**, 1653–1659 (2011).

60. J. Suh, H. Hutter, A survey of putative secreted and transmembrane proteins encoded in the *C. elegans* genome. *BMC Genomics* **13**, 333 (2012).

61. J. D. McGhee, The Caenorhabditis elegans intestine. *Wiley Interdiscip. Rev. Dev. Biol.* **2**, 347–367 (2013).

62. C. Coburn, D. Gems, The mysterious case of the *C. elegans* gut granule: Death anthranilic acid and the kynurenine pathway. *Front. Genet.* **4**, 151 (2013).

63. B. J. Thomas, I. E. Wight, W. Y. Y. Chou, M. Moreno, Z. Dawson, A. Homayouni, H. Huang, H. Kim, H. Jia, J. R. Buland, J. A. Wambach, F. S. Cole, S. C. Pak, G. A. Silverman, C. J. Luke, CemOrange2 fusions facilitate multifluorophore subcellular imaging in *C. elegans*. *PLOS ONE* **14**, 1–25 (2019).

64. C. Fucci, M. Resnati, E. Riva, T. Perini, E. Ruggieri, U. Orfanelli, F. Paradiso, F. Cremasco, A. Raimondi, E. Pasqualetto, M. Nuvolone, L. Rampoldi, S. Cenci, E. Milan, The interaction

of the tumor suppressor FAM46C with p62 and FNDC3 proteins Integrates protein and secretory homeostasis. *Cell Rep.* **32**, 108162 (2020).

65. N. Manfrini, M. Mancino, A. Miluzio, S. Oliveto, M. Balestra, P. Calamita, R. Alfieri, R. L. Rossi, M. Sassoe-Pognetto, C. Salio, A. Cuomo, T. Bonaldi, M. Manfredi, E. Marengo, E. Ranzato, S. Martinotti, D. Cittaro, G. Tonon, S. Biffo, FAM46C and FNDC3A are multiple myeloma tumor suppressors that act in concert to impair clearing of protein aggregates and autophagy. *Cancer Res.* **80**, 4693–4706 (2020).

66. R. A. Zabinsky, B. M. Weum, M. Cui, M. Han, RNA binding protein vigilin collaborates with miRNAs to regulate gene expression for Caenorhabditis elegans larval development. *G3 (Bethesda)* **7**, 2511–2518 (2017).

67. Y. S. Ooi, K. Majzoub, R. A. Flynn, M. A. Mata, J. Diep, J. K. Li, N. van Buuren, N. Rumachik, A. G. Johnson, A. S. Puschnik, C. D. Marceau, L. Mlera, J. M. Grabowski, K. Kirkegaard, M. E. Bloom, P. Sarnow, C. R. Bertozzi, J. E. Carette, An RNA-centric dissection of host complexes controlling flavivirus infection. *Nat. Microbiol.* **4**, 2369–2382 (2019).

68. P. J. Murray, Macrophage polarization. *Annu. Rev. Physiol.* **79**, 541–566 (2017).

69. M. Benoit, B. Desnues, J.-L. Mege, Macrophage polarization in bacterial infections. *J. Immunol.* **181**, 3733–3739 (2008).

70. C. Zheng, Y. C. Ouyang, B. Jiang, X. Lin, J. Chen, M. Z. Dong, X. Zhuang, S. Yuan, Q. Y. Sun, C. Han, Non-canonical RNA polyadenylation polymerase FAM46C is essential for fastening sperm head and flagellum in mice. *Biol. Reprod.* **100**, 1673–1685 (2019).

71. T. Ganz, V. Gabayan, H.-I. Liao, L. Liu, A. Oren, T. Graf, A. M. Cole, Increased inflammation in lysozyme M-deficient mice in response to *Micrococcus luteus* and its peptidoglycan. *Blood* **101**, 2388–2392 (2003).

72. P. Markart, T. R. Korfhagen, T. E. Weaver, H. T. Akinbi, Mouse lysozyme M is important in pulmonary host defense against *Klebsiella pneumoniae* infection. *Am. J. Respir. Crit. Care Med.* **169**, 454–458 (2004).

73. H. T. Akinbi, R. Epaud, H. Bhatt, T. E. Weaver, Bacterial killing is enhanced by expression of lysozyme in the lungs of transgenic mice. *J. Immunol.* **165**, 5760–5766 (2000).

74. A. M. Cole, D. R. Thapa, V. Gabayan, H.-I. Liao, L. Liu, T. Ganz, Decreased clearance of Pseudomonas aeruginosa from airways of mice deficient in lysozyme M. *J. Leukoc. Biol.* **78**, 1081–1085 (2005).

75. E. del Cerro-Vadillo, F. Madrazo-Toca, E. Carrasco-Marín, L. Fernandez-Prieto, C. Beck, F. Leyva-Cobián, P. Saftig, C. Alvarez-Dominguez, Cutting edge: A novel nonoxidative phagosomal mechanism exerted by cathepsin-D controls *Listeria monocytogene*s intracellular growth. *J. Immunol.* **176**, 1321–1325 (2006).

76. Q. Fu, J. Yuan, L. Wang, H. Ran, F. Li, F. Liu, J. Zhang, W. Liu, W. Huang, Y. Huang, X. Xia, Proteomic analysis of murine macrophages mitochondria and lysosomes reveal Cathepsin D as a potential broad-spectrum antimicrobial protein. *J. Proteomics* **223**, 103821 (2020).

77. S.-D. Ha, A. Martins, K. Khazaie, J. Han, B. M. C. Chan, S. O. Kim, Cathepsin B is involved in the trafficking of TNF-α-containing vesicles to the plasma membrane in macrophages. *J. Immunol.* **181**, 690–697 (2008).

78. R. Elling, J. Chan, K. A. Fitzgerald, Emerging role of long noncoding RNAs as regulators of innate immune cell development and inflammatory gene expression. *Eur. J. Immunol.* **46**, 504–512 (2016).

79. M. K. Atianand, D. R. Caffrey, K. A. Fitzgerald, Immunobiology of long noncoding RNAs. *Annu. Rev. Immunol.* **35**, 177–198 (2017).

80. J. Blin, K. A. Fitzgerald, Perspective: The RNA exosome, cytokine gene regulation and links to autoimmunity. *Cytokine* **74**, 175–180 (2015).

81. C. Kew, W. Huang, J. Fischer, R. Ganesan, N. Robinson, A. Antebi, Evolutionarily conserved regulation of immunity by the splicing factor RNP-6/PUF60. *eLife* **9**, 1–23 (2020).

82. A. O. Olaitan, A. Aballay, Non-proteolytic activity of 19S proteasome subunit RPT-6 regulates GATA transcription during response to infection. *PLOS Genet.* **14**, e1007693 (2018).

83. V. Tiku, C. Kew, P. Mehrotra, R. Ganesan, N. Robinson, A. Antebi, Nucleolar fibrillarin is an evolutionarily conserved regulator of bacterial pathogen resistance. *Nat. Commun.* **9**, 1–10 (2018).

84. C.-W. Wu, K. Wimberly, A. Pietras, W. Dodd, M. B. Atlas, K. P. Choe, RNA processing errors triggered by cadmium and integrator complex disruption are signals for environmental stress. *BMC Biol.* **17**, 56 (2019).

85. R. Kaletsky, R. S. Moore, G. D. Vrla, L. R. Parsons, Z. Gitai, C. T. Murphy, *C. elegans* interprets bacterial non-coding RNAs to learn pathogenic avoidance. *Nature* **586**, 445–451 (2020).

86. B. A. Kudlow, L. Zhang, M. Han, Systematic analysis of tissue-restricted miRISCs reveals a broad role for microRNAs in suppressing basal activity of the *C. elegans* pathogen response. *Mol. Cell* **46**, 530–541 (2012).

87. Z. Ren, V. R. Ambros, *Caenorhabditis elegans* microRNAs of the let-7 family act in innate immune response circuits and confer robust developmental timing against pathogen stress. *Proc. Natl. Acad. Sci. U.S.A.* **112**, E2366–E2375 (2015).

88. L. Sun, L. Zhi, S. Shakoor, K. Liao, D. Wang, microRNAs involved in the control of innate immunity in Candida infected *Caenorhabditis elegans*. *Sci. Rep.* **6**, 36036 (2016).

89. J. Le Pen, H. Jiang, T. Di Domenico, E. Kneuss, J. Kosałka, C. Leung, M. Morgan, C. Much, K. L. M. Rudolph, A. J. Enright, D. O'Carroll, D. Wang, E. A. Miska, Terminal uridylyltransferases target RNA viruses as part of the innate immune system. *Nat. Struct. Mol. Biol.* **25**, 778–786 (2018).

90. C. E. Richardson, T. Kooistra, D. H. Kim, An essential role for XBP-1 in host protection against immune activation in *C. elegans*. *Nature* **463**, 1092–1095 (2010).

91. E. J. Tillman, C. E. Richardson, D. J. Cattie, K. C. Reddy, N. J. Lehrbach, R. Droste, G. Ruvkun, D. H. Kim, Endoplasmic reticulum homeostasis is modulated by the forkhead transcription factor FKH-9 during infection of *Caenorhabditis elegans*. *Genetics* **210**, 1329–1337 (2018).

92. E. Vidak, U. Javoršek, M. Vizovišek, B. Turk, Cysteine cathepsins and their extracellular roles: Shaping the microenvironment. *Cell* **8**, 264 (2019).

93. K. Lasocki, A. A. Bartosik, J. Mierzejewska, C. M. Thomas, G. Jagura-Burdzy, Deletion of the parA (soj) homologue in *Pseudomonas aeruginosa* causes ParB instability and affects growth rate, chromosome segregation, and motility. *J. Bacteriol.* **189**, 5762–5772 (2007).

94. A. Paix, A. Folkmann, D. Rasoloson, G. Seydoux, High efficiency, homology-directed genome editing in *Caenorhabditis elegans* using CRISPR-Cas9 ribonucleoprotein complexes. *Genetics* **201**, 47–54 (2015).

95. D. J. Dickinson, A. M. Pani, J. K. Heppert, C. D. Higgins, B. Goldstein, Streamlined genome engineering with a self-excising drug selection cassette. *Genetics* **200**, 1035–1049 (2015).

96. M. R. Green, J. Sambrook, *Molecular Cloning: A Laboratory Manual* (CSH Press, ed. 4, 2012).

97. J. Y. Jeong, H. S. Yim, J. Y. Ryu, H. S. Lee, J. H. Lee, D. S. Seen, S. G. Kang, One-step sequence-and ligation-independent cloning as a rapid and versatile cloning method for functional genomics Studies. *Appl. Environ. Microbiol.* **78**, 5440–5443 (2012).

98. M. Z. Li, S. J. Elledge, SLIC: A method for sequence- and ligation-independent cloning. *Methods Mol. Biol.* **852**, 51–59 (2012).

99. D. Graczyk, R. J. White, K. M. Ryan, Involvement of RNA polymerase III in immune responses. *Mol. Cell. Biol.* **35**, 1848–1859 (2015).

100. J. Pei, B. H. Kim, N. V. Grishin, PROMALS3D: A tool for multiple protein sequence and structure alignments. *Nucleic Acids Res.* **36**, 2295–2300 (2008).

101. R. C. Edgar, MUSCLE: A multiple sequence alignment method with reduced time and space complexity. *BMC Bioinformatics* **5**, 113 (2004).

102. I. Letunic, P. Bork, Interactive tree of life (iTOL) v4: Recent updates and new developments. *Nucleic Acids Res.* **47**, W256–W259 (2019).

103. J. Schindelin, I. Arganda-Carreras, E. Frise, V. Kaynig, M. Longair, T. Pietzsch, S. Preibisch, C. Rueden, S. Saalfeld, B. Schmid, J.-Y. Tinevez, D. J. White, V. Hartenstein, K. Eliceiri, P. Tomancak, A. Cardona, Fiji: An open-source platform for biological-image analysis. *Nat. Methods* **9**, 676–682 (2012).

104. M. Chekulaeva, H. Mathys, J. T. Zipprich, J. Attig, M. Colic, R. Parker, W. Filipowicz, miRNA repression involves GW182-mediated recruitment of CCR4-NOT through conserved W-containing motifs. *Nat. Struct. Mol. Biol.* **18**, 1218–1226 (2011).

105. M. Martin, Cutadapt removes adapter sequences from high-throughput sequencing reads. *EMBnet. J.* **17**, 10 (2011).

106. A. Dobin, C. A. Davis, F. Schlesinger, J. Drenkow, C. Zaleski, S. Jha, P. Batut, M. Chaisson, T. R. Gingeras, STAR: Ultrafast universal RNA-seq aligner. *Bioinformatics* **29**, 15–21 (2013).

107. Y. Liao, G. K. Smyth, W. Shi, FeatureCounts: An efficient general purpose program for assigning sequence reads to genomic features. *Bioinformatics* **30**, 923–930 (2014).

108. M. I. Love, W. Huber, S. Anders, Moderated estimation of fold change and dispersion for RNA-seq data with DESeq2. *Genome Biol.* **15**, 550 (2014).

109. D. Angeles-Albores, R. Y. Raymond, J. Chan, P. W. Sternberg, Tissue enrichment analysis for C. elegans genomics. *BMC Bioinformatics* **17**, 366 (2016).

110. A. D. Holdorf, D. P. Higgins, A. C. Hart, P. R. Boag, G. J. Pazour, A. J. M. Walhout, A. K. Walker, WormCat: An online tool for annotation and visualization of *Caenorhabditis elegans* genome-scale data. *Genetics* **214**, 279–294 (2020).

111. H. Li, Minimap2: Pairwise alignment for nucleotide sequences. *Bioinformatics* **34**, 3094–3100 (2018).

112. R. E. Workman, A. D. Tang, P. S. Tang, M. Jain, J. R. Tyson, R. Razaghi, P. C. Zuzarte, T. Gilpatrick, A. Payne, J. Quick, N. Sadowski, N. Holmes, J. G. de Jesus, K. L. Jones, C. M. Soulette, T. P. Snutch, N. Loman, B. Paten, M. Loose, J. T. Simpson, H. E. Olsen, A. N. Brooks, M. Akeson, W. Timp, Nanopore native RNA sequencing of a human poly(A) transcriptome. *Nat. Methods* **16**, 1–37 (2019).

113. U. Raudvere, L. Kolberg, I. Kuzmin, T. Arak, P. Adler, H. Peterson, J. Vilo, g:Profiler: A web server for functional enrichment analysis and conversions of gene lists (2019 update). *Nucleic Acids Res.* **47**, W191–W198 (2019).

114. A. R. Quinlan, I. M. Hall, BEDTools: A flexible suite of utilities for comparing genomic features. *Bioinformatics* **26**, 841–842 (2010).

115. J. R. Wiśniewski, P. Ostasiewicz, M. Mann, High recovery FASP applied to the proteomic analysis of microdissected formalin fixed paraffin embedded cancer tissues retrieves known colon cancer markers. *J. Proteome Res.* **10**, 3040–3049 (2011).

116. J. Cox, M. Mann, MaxQuant enables high peptide identification rates, individualized p.p.b.-range mass accuracies and proteome-wide protein quantification. *Nat. Biotechnol.* **26**, 1367–1372 (2008).

117. R Core Team, R: A language and environment for statistical computing (2020).

118. Y. Perez-Riverol, A. Csordas, J. Bai, M. Bernal-Llinares, S. Hewapathirana, D. J. Kundu, A. Inuganti, J. Griss, G. Mayer, M. Eisenacher, E. Pérez, J. Uszkoreit, J. Pfeuffer, T. Sachsenberg, Ş. Yilmaz, S. Tiwary, J. Cox, E. Audain, M. Walzer, A. F. Jarnuczak, T.

Ternent, A. Brazma, J. A. Vizcaíno, The PRIDE database and related tools and resources in 2019: Improving support for quantification data. *Nucleic Acids Res.* **47**, D442–D450 (2019).

119. C. Frøkjaer-Jensen, M. W. Davis, C. E. Hopkins, B. J. Newman, J. M. Thummel, S.-P. Olesen, M. Grunnet, E. M. Jorgensen, Single-copy insertion of transgenes in *Caenorhabditis elegans. Nat. Genet.* **40**, 1375–1383 (2008).

120. D. J. Dickinson, J. D. Ward, D. J. Reiner, B. Goldstein, Engineering the *Caenorhabditis elegans* genome using Cas9-triggered homologous recombination. *Nat. Methods* **10**, 1028–1034 (2013).

121. G. J. Woodhead, C. A. Mutch, E. C. Olson, A. Chenn, Cell-autonomous β-catenin signaling regulates cortical precursor proliferation. *J. Neurosci.* **26**, 12620–12630 (2006).